npg

Metabolic stress promotes renal tubular inflammation by triggering the unfolded protein response

S Fougeray[1], N Bouvier[1], P Beaune[1,3], C Legendre[2], D Anglicheau[1,2], E Thervet[1,2] and N Pallet*[1,2]

The renal epithelium contributes to the development of inflammation during ischemic injury. Ischemia induces endoplasmic reticulum (ER) stress and activates the unfolded protein response (UPR). Ischemic tissues generate distress signals and inflammation that activates fibrogenesis and may promote adaptive immunity. Interestingly, the UPR may activate inflammation pathways. Our aim was to test whether the UPR is activated during metabolic stress and mediates a tubular inflammatory response. Glucose deprivation, not hypoxia and amino acids deprivation, activated the UPR in human renal cortical tubular cells in culture. This stress activated NF-κB and promoted the transcription of proinflammatory cytokines and chemokines, including IL-6, IL-8, TNF-α, RANTES and MCP-1. The protein kinase RNA (PKR)-like ER kinase signaling pathway was not required for the induction of inflammation but amplified cytokine. Inositol-requiring enzyme 1 activated NF-κB signaling and was required for the transcription of proinflammatory cytokines and chemokines following metabolic stress. Moreover, acute ischemia activated ER stress and inflammation in rat kidneys. Finally, the ER stress marker GRP78 and NF-κB p65/RelA were coexpressed in human kidney transplants biopsies performed before implantation, suggesting that ER stress activates tubular inflammation in human renal allografts. In conclusion, this study establishes a link between ischemic stress, the activation of the UPR and the generation of a tubular inflammatory response.
Cell Death and Disease (2011) **2**, e143; doi:10.1038/cddis.2011.26; published online 14 April 2011
Subject Category: Immunity

Ischemia, the shortage of blood supply into an organ is a common complication of various clinical conditions including cancer, stroke or solid organ transplantation. Renal ischemia is a major cause of acute and end-stage renal failure, which causes serious morbidity and mortality.[1] In the renal transplant setting, ischemic injuries under toxic conditions (calcineurin inhibitors), surgical pressure or immunological injury compromise tissue viability and promote alloimmunity, leading to interstitial fibrosis/tubular atrophy, progressive graft dysfunction and loss.[2,3] In addition, acute ischemia in native kidneys may trigger autoimmunity through the generation of alarm signals by stressed and/or dying cells and the generation of endogenous neoantigens and epitope spreading.[4–6]

The renal tubular epithelium has a central role in the development of acute and chronic kidney structural deterioration after ischemic injury, especially by the generation of inflammatory and profibrogenic cytokines.[7,8] Renal ischemia generates a cascade of proinflammatory mediators that can amplify injury. For example, renal-associated TLRs 2 and 4 recognize danger-associated molecular patterns (DAMPs) and promote local inflammation.[9,10] Modulation of the graft microenvironment by this early innate response may be a prerequisite for fibrogenesis and for the full development of adaptive immunity and subsequent renal allograft rejection.

The primary mechanism through which the ischemic kidney initiates this inflammatory cascade has not yet been fully elucidated and alternative biological pathways should be tested. Although various extracellular stimuli, including DAMPs, promote tubular inflammation, the implication of intracellular distress processes on tubular inflammation remains to be determined.

Tubular cells that encounter nutrient and oxygen deprivation during ischemia use various adaptive responses to maintain homeostasis and survival, including the inhibition of degradation of hypoxia inducible factor-1α, the inhibition of mammalian target of rapamycin-dependent signaling and the initiation of macroautophagy and the activation of the unfolded protein response (UPR). These adaptive responses decrease energy expenditure, increase nutrient availability and promote cell survival. However, these biological processes also lead to the generation of proinflammatory cytokines and chemokines, suggesting that stressed tissues generate alarm signals that produce an inflammatory microenvironment in addition to releasing DAMPs.[11–14] Whether such responses trigger inflammation in the setting of acute renal ischemia is unknown.

Ischemia promotes endoplasmic reticulum (ER) stress, a situation that is caused by the accumulation of misfolded

---

[1]INSERM U775, Université Paris Descartes, Paris, France; [2]Service de Transplantation Rénale, Hôpital Necker, Paris, France and [3]Pôle de Biologie, Hôpital Européen Georges Pompidou, Paris, France
*Corresponding author: N Pallet, INSERM U775, Centre Universitaire des Saints Pères. 45 rue des Saints-Pères, Paris 75006, France. Tel: + 33 14 286 2251; Fax: + 33 14 286 2072; E-mail: nicolas.pallet@nck.aphp.fr

proteins in the lumen of the ER. ATP shortage caused by hypoxia and glucose deprivation decreases the intra-reticular calcium concentration, impairs the activity of chaperone molecules, interferes with disulfide bridge formation and impairs the maturation of native proteins.[15–17] The function of the UPR is to adjust cell functions in response to ER stress and to re-establish normal ER function both at the translational and transcriptional level. If the stress persists and adaptation fails, the cell activates the apoptotic program.[11] In ER stress conditions, the aim of the UPR is to adapt to the changing environment and reestablish normal ER function, by reducing messenger RNA (mRNA) translation and therefore the amount of new synthesized proteins in the ER, by increasing the proteasomal degradation of ER localized proteins, and by increasing the protein folding capacity of the ER. When adaptation fails and ER stress prolongs, cell triggers death programs, usually in the form of apoptosis.[18] Three major mediators are involved in the UPR signaling: activated transcription factor 6 (ATF6), inositol-requiring enzyme 1 (IRE1) and protein kinase RNA (PKR)-like ER kinase (PERK).

The aim of this study was to investigate whether renal tubular cells promote inflammation through the UPR in the context of ischemic injury. We have demonstrated that glucose deprivation, not hypoxia and amino acids shortage induces ER stress and activates the IRE1 and PERK pathways in human renal cortical cells (HRCCs) in culture. Although the IRE1 axis is necessary for NF-κB activation and proinflammatory cytokines production, the PERK pathway is not required for NF-κB activation but amplifies the tubular inflammatory response. Moreover, ER stress and NF-κB are also activated in rat kidneys following acute cold ischemia. Finally, we have demonstrated that acute kidney ischemic injury promotes tubular ER stress and activates the NF-κB pathway in human renal allografts.

Results

Glucose deprivation, not hypoxia and amino acids shortage promote ER stress.

We first examined which metabolic constituent of ischemia, namely glucose or amino acids deprivation, or hypoxia, induced ER stress in tubular cells. HRCCs exposed for 24 h to glucose-deprived culture medium expressed the ER stress marker GRP78, also known as binding immunoglobin protein, whereas cells cultured for 24 h without amino acids, or subjected to hypoxia (Figure 1a, bottom) did not develop ER stress (Figures 1a and c). GRP94, a chaperone involved in the adaptive response to ER stress, was also expressed during glucose deprivation (Figure 1b). These results suggest that glucose deprivation, but not amino acids deprivation or hypoxia, promotes ER stress in HRCCs in culture.

Metabolic stress activates the PERK pathway.

As glucose deprivation, hereafter referred to as metabolic stress, promotes tubular ER stress, we next tested whether the UPR was activated. Metabolic stress activated the PERK pathway, as shown by the early phosphorylation of the translation initiator elongation initiation factor 2α (eIF2α;

Figure 2a), followed by the selectively translated transcriptional factor ATF4 (Figure 2b) and the expression of transcripts for the apoptotic inducers C/EBP homologous protein (CHOP; also known as growth arrest and DNA-damage-inducible protein 153 (GADD153)) and GADD34 (Figure 2c). These results suggest that metabolic stress activates the PERK pathway in HRCCs.

Metabolic stress activates the IRE1 pathway.

IRE1 homodimerizes during ER stress and acquires kinase and endonuclease activities. In HRCCs subjected to metabolic stress, the transcriptional factor X-box-binding protein 1 (XBP1) was actively spliced during glucose deprivation (Figure 2d), suggesting that IRE1 is activated during metabolic stress. Together, these results indicate that metabolic stress activates IRE1 signaling in HRCCs.

Metabolic stress generates a tubular inflammatory response.

We next tested whether metabolic stress could promote tubular inflammation. We evaluated the expression of various proinflammatory cytokine and chemokine transcripts during metabolic stress. These transcripts are expressed during acute kidney injury.[4] HRCCs exposed to metabolic stress showed biphasic expression patterns for IL-6, IL-8, TNF-α, MCP-1 and RANTES, whereas CX3CL1 and IL-1β expression did not increase (Figure 3a). IL-6, IL-8, MCP-1 and TNF-α expression levels peaked early, between 2 and 8 h after stimulation, followed by significant expression inhibition beginning after 12 h. RANTES expression profile was different from the other cytokines, as its expression was maintained even after 12 h, time at which the other cytokines were downregulated. Hierarchical clustering of the gene expression profiles suggested that metabolic stress and the ER stress inducer tunicamycin promote similar proinflammatory profiles which are different from that induced by TNF-α (Figure 3a). These results suggest that ER stress (chemically or metabolically induced) and the prototypical proinflammatory cytokine TNF-α generate distinct tubular inflammatory profiles. C/EBPβ, a transcription factor that inhibits the proinflammatory properties of ER stress, was transiently induced by metabolic stress and could, at least in part, be responsible for the biphasic patterns (Figure 3b).

Metabolic stress activates NF-κB signaling.

Inflammatory responses to stress usually involve NF-κB signaling. HRCCs challenged with metabolic stress activated NF-κB signaling. Indeed, the expression of the NF-κB repressor IκBα was transiently reduced (Figure 3c, left) and NF-κB p65/RelA expression was transiently increased during metabolic stress (Figure 3c, right). Moreover, the nuclear translocation of the transcriptional factor NF-κB p65/RelA was observed by immunofluorescence imaging in the same conditions, 2 h after the initiation of the stress (Figure 3d). Taken together, these results suggest that metabolic stress activates the proinflammatory NF-κB pathway. We next hypothesized that the UPR activated during metabolic stress could promote tubular inflammation.
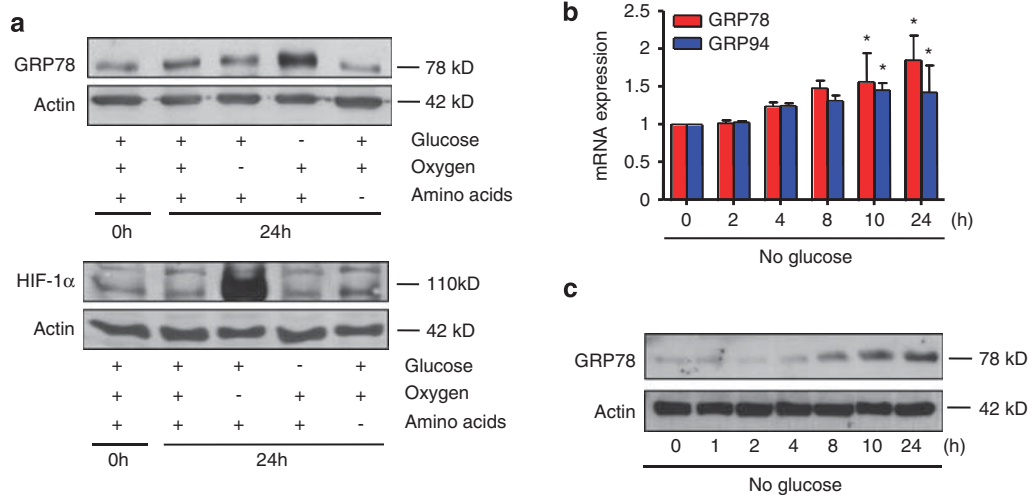
Figure 1 Glucose deprivation, not hypoxia and amino acids shortage promote ER stress. (a) GRP78 and HIF-1α expression during various metabolic stresses. Levels of GRP78 (top) and HIF-1α (bottom) expression are shown from HRCCs incubated in glucose- or amino acids-deficient culture media or challenged with hypoxia for 24 h. A representative immunoblot of three independent experiments is shown. (b) Metabolic stress promotes chaperones genes transcription. HRCCs were cultured in glucose-deprived culture medium for the indicated periods. *GRP78* and *GRP94* transcripts levels, measured by qRT-PCR, are presented as mean ± S.E.M. relative to levels before metabolic stress over three independent experiments. *$P < 0.05$. (c) Metabolic stress promotes time-dependent GRP78 expression. HRCCs were cultured in glucose-deficient medium for the indicated periods and GRP78 protein expression was determined by immunoblotting. A representative immunoblot of three independent experiments is shown
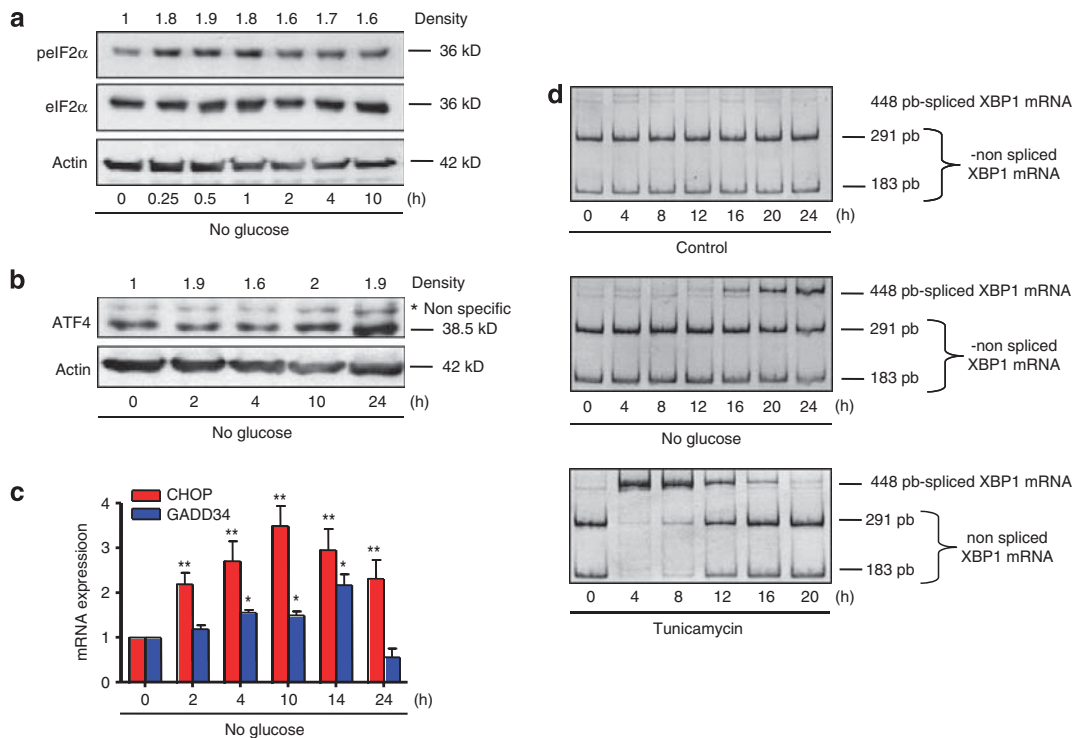

Figure 2 Metabolic stress activates the PERK and IRE1 pathways. (a) eIF2α is phosphorylated during metabolic stress. Phospho-eIF2α expression was evaluated by immunoblotting in HRCCs cultured in glucose-deficient medium for the indicated periods. A representative immunoblot of three independent experiments is shown. Density refers to peIF2α/total eIF2α. (b) ATF4 expression is upregulated during metabolic stress. ATF4 protein expression was evaluated by immunoblotting in HRCCs cultured in glucose-deficient medium for the indicated periods. A representative immunoblot of three independent experiments is shown. (c) *CHOP* and *GADD34* transcripts expression is upregulated under metabolic stress. HRCCs were cultured in glucose-deficient medium for the indicated periods. Transcripts levels, measured by qRT-PCR, are presented as the mean ± S.E.M. relative to the levels before metabolic stress for three independent experiments. *$P < 0.05$; **$P < 0.01$. (d) Metabolic stress promotes XBP1 splicing. HRCCs were subjected to a time course of tunicamycin (2 μg/ml) exposure or cultured in glucose-deficient medium for the indicated periods. *XBP1* mRNA splicing was examined by PCR and followed by migration in polyacrylamide gels. See the Material and Methods section for more details
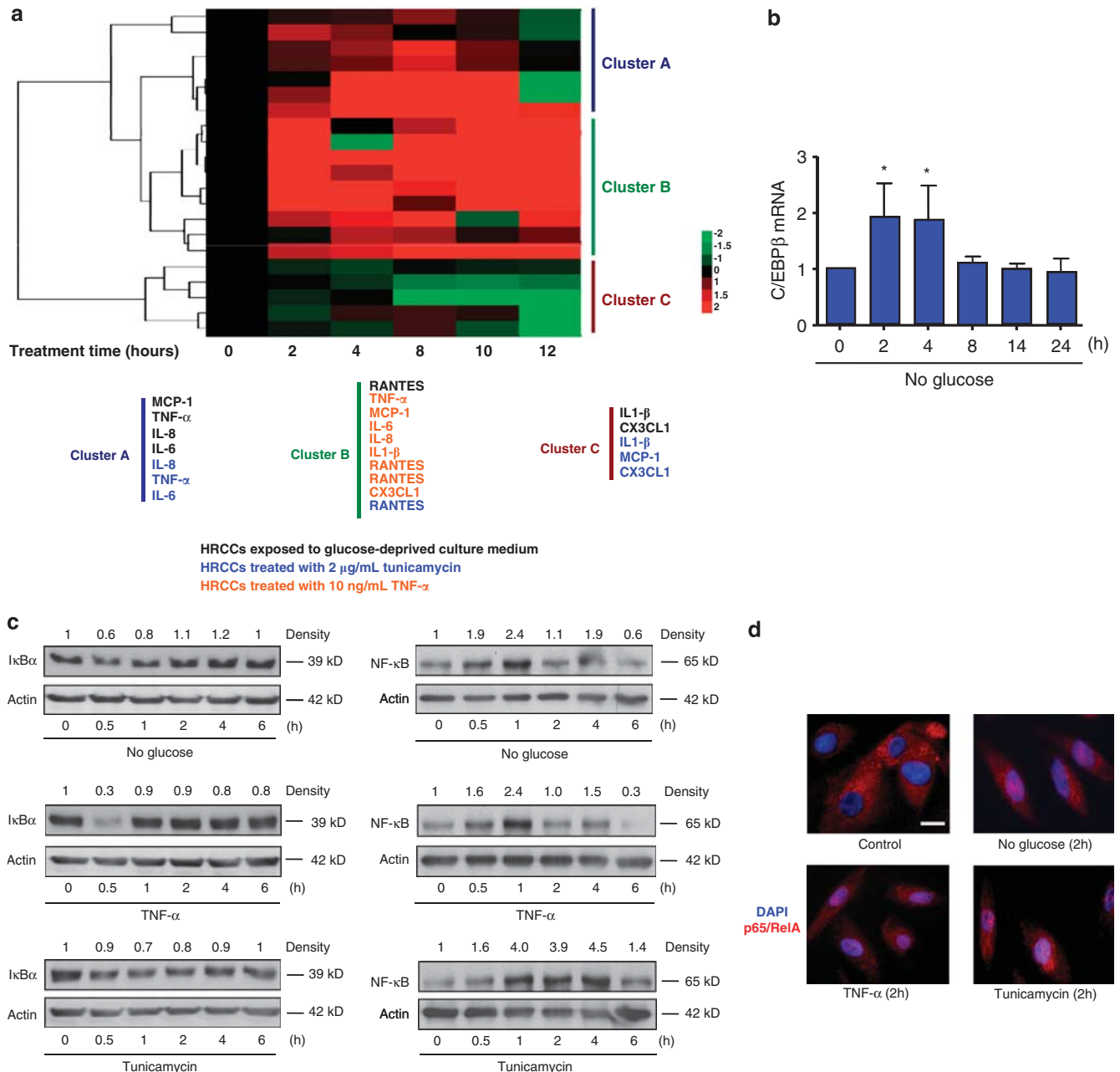
Figure 3 Metabolic stress generates a tubular inflammatory response and activates NF-κB signaling. (**a**) Heat Map of cytokines expression profiles. HRCCs were cultured in glucose-deficient medium or incubated with tunicamycin (2 μg/ml) or TNF-α (10 ng/ml). *IL-6, IL-8, TNF-α, MCP-1, RANTES, CX3CL1* and *IL-1β* transcripts levels were measured by qRT-PCR. Expression levels shown are representative of the $2_t^{-\Delta\Delta C}$ obtained from eight independent replicates at each time point. Time resolved supervised hierarchical clustering of transcripts expression was performed. The brightness of the green and red represents the degree to which expression was lower or higher, respectively, in the HRCCs relative to cells before treatment. (**b**) C/EBPβ is transiently upregulated during metabolic stress. HRCCs were cultured in glucose-deficient medium. *C/EBPβ* transcripts levels were measured by qRT-PCR and are presented as the mean ± S.E.M. relative to levels in cells before treatment for three independent experiments. (**c**) IκBα is degraded and NF-κB p65/RelA expression is increased during metabolic stress. Protein expression of IκBα (left) and NF-κB p65/RelA (right) in HRCCs cultured in glucose-deficient medium or incubated with 10 ng/ml TNF-α or 2 μg/ml tunicamycin for the indicated periods was evaluated. A representative immunoblot of three independent experiments is shown. (**d**) NF-κB p65/RelA translocates in the nucleus during metabolic stress. NF-κB p65/RelA nuclear translocation was evaluated by immunofluorescence analysis. HRCCs were cultured in glucose-deficient medium or incubated with 10 ng/ml TNF-α or 2 μg/ml tunicamycin for 2 h. Cells were counterstained with DAPI to visualize the nuclei. White bar = 10 μm. A representative picture of three independent experiments is shown

The PERK pathway is not required for triggering tubular inflammation during metabolic stress. We transiently inhibited PERK signaling during metabolic stress by RNA interference using synthetic small interfering RNA (siRNA) directed against the PERK mRNA (Figure 4a). PERK

inhibition did not seem to alter NF-κB signaling because the IκBα expression profiles were similar during metabolic stress with or without PERK knockdown (Figure 4b). PERK inhibition did not alter cytokines expression profiles (not shown). This result suggests that the PERK pathway is not
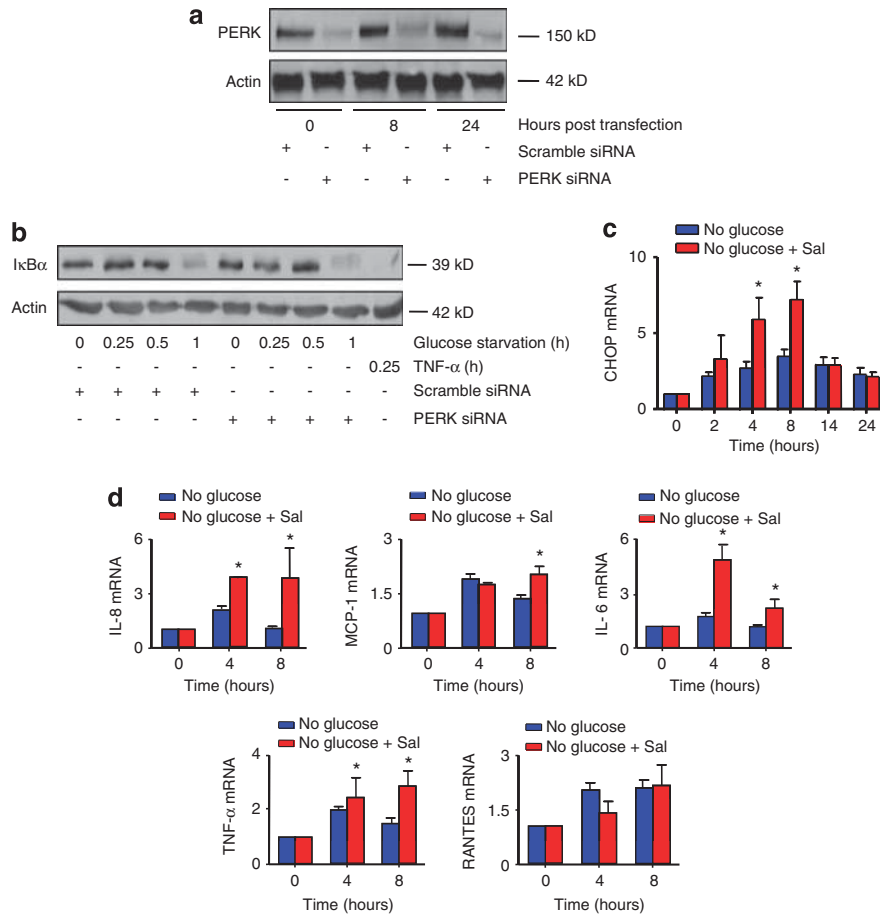
Figure 4 PERK is not required for triggering tubular inflammation during metabolic stress. (**a**) RNA interference directed against *PERK* transcripts. HRCCs were transfected with siRNA targeting *PERK* transcripts or control non-targeting (scramble) siRNAs. At 24 h post transfection, cells were incubated with glucose-free medium and the PERK protein level was measured at different periods of time. A representative analysis of PERK by immunoblotting is shown (*n* = 3). (**b**) PERK inhibition does not reduce IκBα degradation during metabolic stress. IκBα protein levels are shown in HRCCs transfected with either PERK or scramble siRNA or control cells. At 24 h post transfection, cells were incubated for 1 h with glucose-deficient medium or incubated with 10 ng/ml TNF-α for 15 min. An immunoblot representative of three independent experiments is shown. (**c**) Salubrinal amplifies PERK signaling during metabolic stress. HRCCs were incubated with glucose-deficient medium for various periods of time with or without 20 μM salubrinal. *CHOP* transcripts were measured by qRT-PCR after different periods of time. Transcripts expression levels are presented as the mean ± S.E.M. relative to the levels in non-treated cells and are representative of three independent experiments. *$P < 0.05$. (**d**) Salubrinal amplifies tubular inflammation during metabolic stress. HRCCs were incubated with glucose-free medium for various periods of time with 20 μM salubrinal. *IL-6, IL-8, TNF-α, RANTES* and *MCP-1* transcripts were measured by qRT-PCR after different periods of time. Transcripts expression levels are presented as the mean ± S.E.M. relative to levels in control cells and are representative of three independent experiments. *$P < 0.05$

required for the initiation of tubular inflammation during metabolic stress. To activate the PERK pathway, we incubated HRCCs with salubrinal, a molecule that selectively blocks eIF2á dephosphorylation via inhibiting the serine/ threonine phosphatase PP1 and amplifies the activation of the PERK pathway, among other effects. Salubrinal promoted the activation of the PERK pathway, as exemplified by the overexpression of CHOP during metabolic stress (Figure 4c). Salubrinal also amplified the expression of proinflammatory cytokines and chemokines (but not RANTES) during metabolic stress (Figure 4d). Together, these results suggest that PERK signaling during metabolic stress does not seem to be required for mediating tubular inflammation but could constitute an accessory pathway that promotes tubular inflammation when selectively activated.

The IRE1 pathway mediates tubular inflammation during metabolic stress. We next focused on IRE1 signaling

during metabolic stress. IRE1 inhibition was effective after siRNA transfection (Figure 5a). Regarding NF-κB signaling, IRE1 inhibition reduced IκBα degradation, NF-κB p65/RelA increase and NF-κB p65/RelA nuclear translocation during metabolic stress (Figure 5b). IRE1 inhibition was associated with reduced expression levels of proinflammatory cytokines during metabolic stress, including IL-8, RANTES, TNF-α and IL-6 to a lesser extend (Figure 5c). MCP-1 expression during metabolic stress did not seem to depend on IRE1 signaling (data not shown). These experiments suggest that metabolic stress generates tubular inflammation that is in part mediated by IRE1-dependent NF-κB signaling.

Cold ischemia in rat kidneys induces ER stress and promotes inflammation. To translate our *in vitro* findings to an *in vivo* setting, we reproduced cold ischemia conditions encountered during kidney transplantation and analyzed
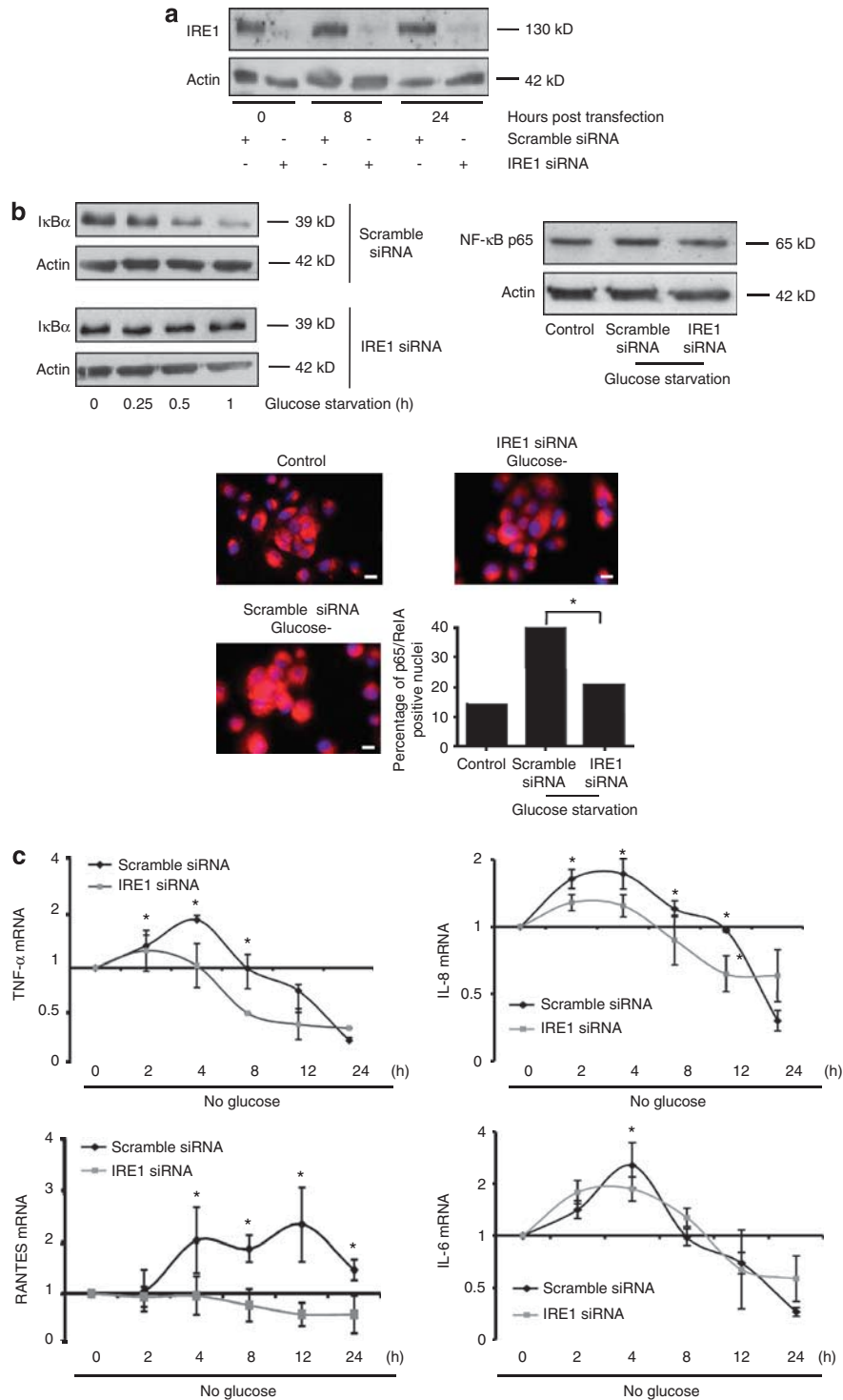
Figure 5 IRE1 mediates tubular inflammation during metabolic stress. (**a**) RNA interference directed against *IRE1* transcripts. HRCCs were transfected with siRNA targeting *IRE1* transcripts or control non-targeting (scramble) siRNAs. At 24 h post transfection, cells were incubated with glucose-free medium and the IRE1 protein level was measured at different periods of time. A representative analysis of IRE1 by immunoblotting is shown ($n = 3$). (**b**) IRE1 inhibition inhibits NF-κB activation during metabolic stress. Left: IκBα protein levels are shown in HRCCs transfected with either IRE1 or scramble siRNA. At 24 h after transfection, cells were incubated for 1 h with glucose-free medium. An immunoblot representative of three independent experiments is shown. Right: NF-κB p65 protein levels are shown in HRCCs transfected with either IRE1 or scramble siRNA. At 24 h after transfection, cells were incubated for 1 h with glucose-free medium. An immunoblot representative of three independent experiments is shown. Bottom: NF-κB p65/RelA nuclear translocation was evaluated by immunofluorescence analysis. HRCCs transfected with either IRE1 or scramble siRNA were cultured for 2 h in glucose-deficient medium. Cells were counterstained with DAPI (blue) to visualize the nuclei. White bar = 10 μm. Nuclear NF-κB p65/RelA (red) staining is quantified by dividing the number of positive cells by the total number of cells at magnification $\times$ 10. (**c**) IRE1 inhibition reduces tubular inflammation during metabolic stress. HRCCs were transfected with siRNA targeting *IRE1* transcripts or control non-targeting (scramble) siRNAs. At 24 h post transfection, cells were incubated with glucose-free medium and *IL-8*, *IL-6*, *TNF-α* and *RANTES* transcripts were measured by qRT-PCR at different periods of time. Transcripts expression levels are presented as a mean $\pm$ S.E.M. relative to levels in cells transfected with control siRNA and are representative of three independent experiments. *$P < 0.05$
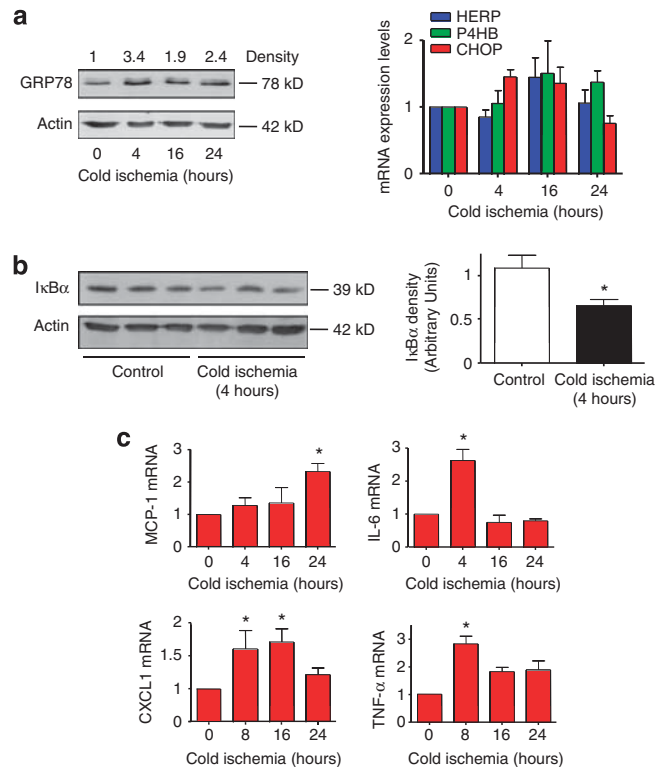
Figure 6 Cold ischemia in rat kidneys activates ER stress and generates an inflammatory response. (**a**) Cold ischemia promotes endoplasmic reticulum stress in rat kidneys. Rats were nephrectomized and kidneys were rinsed and incubated in an IGL1 solution for up to 24 h. Left: GRP78 protein levels in rat kidneys after various times of cold ischemia were measured. A representative immunoblot is shown. Right: expression levels of the *HERP*, *P4HB* and *CHOP* transcripts in rat kidneys after 0, 4, 16 or 24 h of cold ischemia were measured by qRT-PCR. Expression levels are presented as the mean ± S.E.M. relative to the levels in rat kidneys before cold ischemia, $n = 4$ per group. (**b**) Cold ischemia promotes IκBα degradation in rat kidneys. IκBα protein levels in rat kidneys after 4 h of cold ischemia were measured. A representative immunoblot and densitometric analysis are shown. (**c**) Cold ischemia promotes inflammation in rat kidneys. *IL-6*, *TNF-α*, *MCP-1* and *CXCL1* transcripts expression levels in rat kidneys after various times of cold ischemia were measured by qRT-PCR. Expression levels are presented as the mean ± S.E.M. relative to the levels in rat kidneys before cold ischemia, $n = 4$ per group. *$P < 0.05$

whether acute ischemia produces ER stress and inflammation in rat kidneys. Rats were nephrectomized and kidneys were conserved in IGL1 (Institute Geroges Lopez, Lyon, France) at 4 °C for various periods of time. The ER stress surrogate marker GRP78 was expressed as early as at 4 h after nephrectomy and was maintained after 24 h (Figure 6a, left). The expression levels of other ER stress markers including CHOP, protein disulfide isomerase and HERP were also increased during acute ischemia (Figure 6a, right). These results suggest that ER stress and the UPR are activated in rat kidneys during acute ischemia. We next characterized the inflammatory processes in ischemic rats kidneys. IκBα expression was downregulated following cold ischemia, suggesting that NF-κB signaling is activated in the cortex of ischemic kidneys (Figure 6b). Kidney ischemia promoted expression cytokines, including IL-6, TNF-α, MCP-1 and the neutrophil chemoattractant CXCL1, a murin homolog of human IL-8 (Figure 6c). Whether ER stress is directly responsible the kidney inflammation during 'cold' ischemia *in vivo* remains to be definitely demonstrated, but our results strongly suggest that these two processes are linked.

ER stress and NF-κB activation are associated in renal allograft biopsies. Finally, we performed an immuno-histological study in 18 preimplantation human renal

allograft biopsies to investigate whether ER stress and NF-κB activation are present after acute ischemia. These biopsies were performed just before the kidney transplantation and constitute an interesting human model of acute ischemia. We compared the expression levels of GRP78 between these samples and 15 control biopsies performed at 3 months post transplant in stable patients with a normal renal function. Living donor kidneys were excluded. The mean ± S.E.M. cold ischemia time was 18 ± 3 h. Control biopsies displayed a low, if not, tubular GRP78 staining; in preimplantation biopsies a strong perinuclear staining was observed (Figure 7a), suggesting that cold ischemia induces ER stress in renal allografts before transplantation. The semiquantitative evaluation showed that GRP78 expression is significantly higher in the preimplantation group than the control group (Figure 7a). In the same manner, NF-κB p65/ RelA nuclear staining was found in the preimplantation group, whereas the control group displayed weak staining (Figure 7b). NF-κB p65/RelA nuclear staining was significantly higher in the preimplantation group than in the control group (Figure 7b). Finally, we found that GRP78 and NF-κB p65/RelA colocalized in the same tubules, suggesting that these two processes are linked (please compare preimplantation biopsies on Figures 7a and b). GRP78 and NF-κB p65/RelA colocalized cortical tubular cells, a finding
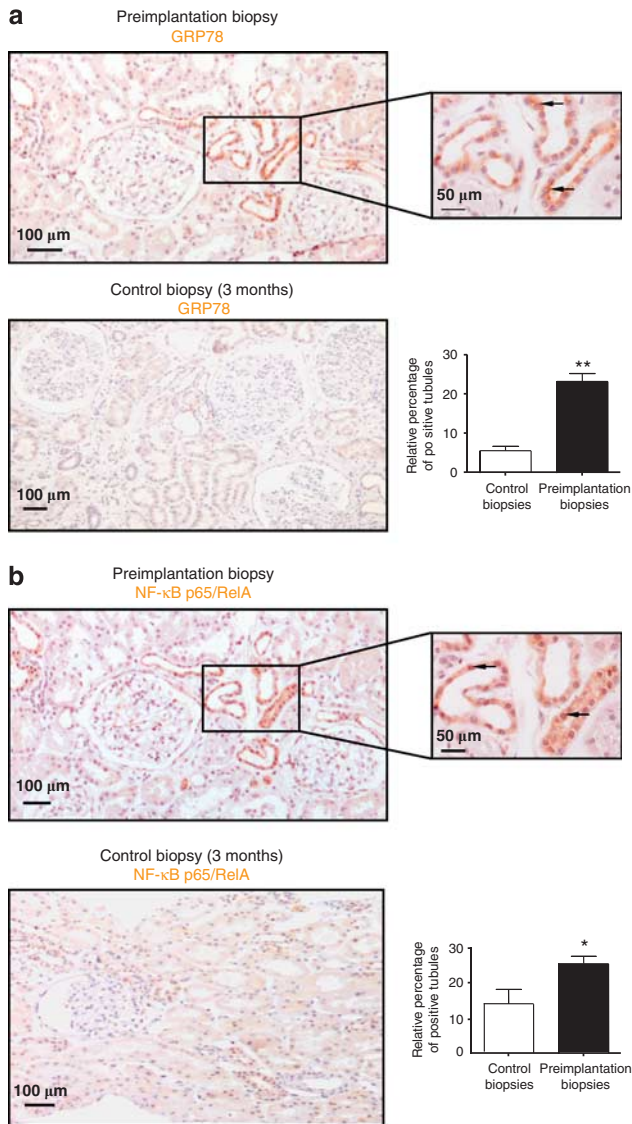
a

Preimplantation biopsy
GRP78

Control biopsy (3 months)
GRP78

b

Preimplantation biopsy
NF-κB p65/RelA

Control biopsy (3 months)
NF-κB p65/RelA

Figure 7 ER stress and NF-κB activation are associated in renal allograft biopsies. (**a**) Tubular expression of GRP78 is upregulated following cold ischemia in human kidney allografts. Left: a representative image of GRP78 immunohisto-chemistry in a preimplantation biopsy with a perinuclear staining (arrows) and a control biopsy. Right: quantification of tubular GRP78 staining in preimplantation biopsies compared with controls (protocol biopsies performed qt 3 months after transplantation). $n = 18$ for preimplantation biopsies and $n = 15$ for the control group. **$P < 0.01$. (**b**) NF-κB signaling is activated following cold ischemia in human kidney allografts. Left: a representative image of NF-κB p65/RelA immuno-histochemistry in preimplantation biopsy with nuclear staining (arrows) and control biopsy. Right: quantification of tubular NF-κB p65/RelA staining in preimplantation biopsies compared with controls (protocol biopsies performed at 3 months after transplantation). $n = 18$ in preimplantation biopsies and $n = 15$ in the control group. *$P < 0.05$

that confirms our in vitro findings on HRCCs. In conclusion, acute kidney ischemic injury promotes tubular ER stress and activates the NF-κB pathway in human renal allografts.

Discussion

Cellular responses to acute kidney ischemia promote profound biological alterations that lead to metabolic

adaptation and cell survival in the injured milieu. Complex biological pathways are activated to reduce cellular energy expenditure, activate anaerobic glycolysis, increase blood supply and nutrient transport and ultimately maintain cell viability. Ischemia induces metabolic stress that is secondary to oxygen, amino acids and glucose deprivation and activates complex evolutionarily conserved responses, including the UPR. Although this adaptive response promotes cell survival and adaptation to metabolic stress, it also generates distress signals that could locally promote inflammation. This concept is important because a proinflammatory microenvironment is known to favor the adaptive immune response.[19] The precise mechanisms by which renal tubular cells initiate this proin-flammatory response remain to be definitively elucidated.

In this study, we identified the UPR as a new factor in the induction of an inflammatory response during metabolic challenge. Tubular epithelial cells may generate a proinflam-matory microenvironment during acute ischemic kidney injury as a consequence of extracellular stimuli including comple-ment activation[20] or activation of TLRs by high-mobility group B1, heat shock proteins, hyaluronans and biglycans.[9,10] Although these studies highlight the important role of epithelial cells in inflammation following acute kidney injury, they rely on the role of above mentioned extracellular mediators. Here we demonstrate that intracellular stress induced by glucose deprivation promotes tubular inflammation generating a proinflammatory microenvironment prone to the development of alloimmunity.

We observed a biphasic profile of NF-κB and cytokines expression during metabolic stress, suggesting that although ER stress may induce proinflammatory molecules via transient activation of NF-κB in the early phase and suppression in later phase. Previous work demonstrated that C/EBPβ, a transcriptional factor whose expression has been shown to increase during ER stress through ill-defined mechanisms, interacts with and inhibits NF-κB during ER stress.[21] As we found that C/EBPβ is expressed during metabolic stress, one can speculate that ER stress is possibly involved not only in the initiation of renal inflammation but also in its resolution. Whether this inhibitory process occurs in vivo and in a human setting remains to be determined. Intriguingly, RANTES expression profile during glucose starvation is different from the other cytokines. There is indeed a biphasic activation of RANTES that persists even after 12 h, time at which the other cytokines evaluated are already down-regulated. The functional significance of these findings for T-cell accumulation at the site of inflammation remains to be demonstrated. Given the chemotactic activity of RANTES that brings T cells, dendritic cells and NK cells to sites of inflammation, one can speculate that RANTES can have detrimental effects via the recruitment of immune cells that enhance inflammatory processes and promote alloimmunity during ischemia.

The detailed mechanisms by which NF-κB is activated under ER stress are poorly understood. The UPR can directly promote NF-κB activation through a PERK–eIF2α-mediated translation attenuation.[22] Because the half-life of IκBα is much shorter than that of NF-κB transcriptional factors, attenuating translation increases the ratio of NF-κB to IκBα and frees NF-κB to translocate to the nucleus in response to ER stress.

In response to ER stress, the autophosphorylation of IRE1 induces a conformational change in its cytosolic domain, which can then bind to the adapter protein tumor necrosis factor-associated receptor 2 (TRAF2). The IRE1α–TRAF2 complex recruit IκB kinase, which phosphorylates IκBα, leading to its degradation and the nuclear translocation of NF-κB.[23] The IRE1α–TRAF2 complex can also recruit the protein kinase JNK, leading to the activation of JNK and the phosphorylation of the transcription factor AP1.[24] Our data suggest that the IRE1 and PERK transducers are different drivers of NF-κB signaling and promote non-redundant cytokine expression profiles. These results are of importance because IRE1 and PERK are differentially activated depending on the cell type, the nature, the intensity and duration of stimuli. Thus, deciphering their respective role in mediating tubular inflammation during ischemic injury could help to better understand the links between ischemic injuries and innate immunity activation.

The UPR is involved in renal tissue response following acute ischemic injury and has a complex role in regulating cell adaptation to stressful conditions and promoting cellular demise.[16,25] Recent studies have suggested that the UPR is responsible for the inhibition of protein synthesis that occurs in rat kidneys after ischemia–reperfusion (IR) and participates in the onset of renal tubular injury.[26,27] Conversely, preconditioning of renal epithelial cells in culture with ER stress inducers protects against oxidative assault (reperfusion) and cytotoxicity, suggesting that the cells were protected from injury if ER stress precedes the ischemic assault.[28] The ambivalent detrimental and cytoprotective properties of the UPR parallel our findings regarding proinflammatory and antiinflammatory properties of the UPR during metabolic stress. Understanding this dynamic process is of great importance to develop nephroprotective strategies that target the UPR.

Our findings should be interpreted in the setting of 'pure' acute ischemia rather than as the consequences of IR because we did not analyze ER stress and inflammation after reperfusion injury. The classical model used to analyze tissue response after acute ischemia is the IR model characterized by the clamping of the renal artery for 30 minutes or more (i.e., warm ischemia) followed by reperfusion. Although widely accepted, this model does not reflect the kind of IR injury that occurs in renal transplantation because that ischemic changes occur in a kidney that has been profusely rinsed and is devoid of blood, and the duration of cold ischemia time can be a few hours to > 30 h. The consequences of these two kinds of ischemia are clinically and biologically different. However, the model we used does not take into account the consequences of the reperfusion injury that are known to produce oxidative stress and is know to trigger ER stress.

In conclusion, we demonstrated that ischemia promotes tubular ER stress and activates the UPR, in vitro, in vivo and in human allograft biopsies collected before kidney implantation. The UPR is involved in mounting an inflammatory tubular response that could help to constitute the proinflammatory microenvironment known to encourage the adaptive immune response.

Materials and Methods

Cell culture. HRCCs were recovered from human nephrectomy specimens and cultured according to previously published methods.[29] Hypoxia experiments were performed using the Anaerocult P kit (Merck, VWR, Fontenay sous Bois, France) following manufacturer instructions. To produce metabolic stress, HRCCs were incubated in a nutrient-deprived culture medium. Nutrient culture medium was DMEM supplemented with 1% fetal calf serum and penicillin–streptomycin.

RNA extraction and RT-PCR. Total RNA was extracted using the RNeasy Mini Kit (Qiagen, Courtaboeuf, France) following the manufacturer's protocol. The yield and purity of RNA were measured using a NanoDrop ND-1000 spectrophotometer (Nanodrop Technologies, Labtech, Palaiseau, France). Transcript expression levels were quantified by SYBR green real-time PCR using an ABI PRISM 7900 sequence detector system (Applied Biosystems, Courtaboeuf, France). Vehicle-treated samples were used as controls, and fold changes for each tested gene were normalized to housekeeping genes (ribosomal protein L13A for in vitro analyses and TATA-box-binding protein for in vivo analyses). The relative expression levels between samples were calculated using the comparative delta C_t (threshold cycle number) method.[30] Primers are listed in Supplemental Table 1.

Protein extraction and western blot analysis. Protein extraction and immunoblotting were performed as previously described.[29] Details on antibodies are listed on Supplemental Table 2.

Immunofluorescence microscopy. HRCCs were cultured on glass coverslips and fixed with 4% paraformaldehyde, rinsed with phosphate-buffered saline and blocked with 2% bovine serum albumin. Cells were permeabilized with Triton X-100 and incubated with a rabbit anti NF-κB p65/RelA antibody. Samples were then incubated with an anti-rabbit Cyanine 3-coupled antibody (Jackson Immunoresearch, Marseille, France). Then, cells were washed and stained with 4′,6-diamidino-2-phenylindole (Vector Laboratories, Peterborough, UK). Slides were mounted and viewed using a Nikon Eclipse TE 2000E (Nikon, Champigny sur Marne, France) imaging fluorescence microscope. Details on antibodies are listed on Supplemental Table 2.

siRNA transfections. PERK, IRE1 and scramble (control) siRNAs were designed and obtained from Qiagen. Transfection was performed using HiPerFect (Qiagen) as the transfection reagent and following the manufacturer protocol.

Analysis of XBP1 processing. HRCCs were exposed to metabolic stress or tunicamycin, and the XBP1 cDNA encompassing the region of restriction site was amplified by PCR using the following primers forward 5′-aaacagagtagcagctca-3′ and reverse 5′-tccttctgggtagacctctgggag-3′ and the PCR product was incubated with the Pst1 restriction enzyme for 1 h at 37 °C, and the restriction digests were separated on a 8% polyacrylamide gel with ethidium bromide. The gels were photographed under UV transillumination and quantified by densitometry. The XBP1 mRNA that was resistant to Pst1 and therefore already spliced and activated was detected as a 448-bp, Pst1−, amplification product, which is indicative of spliced XBP1 mRNA. XBP1 PCR products were digested with Pst1 (Pst1 +), to produce 291-bp and 183-bp amplification products, which indicate a predominance of the native, unspliced form of the XBP1 mRNA.

***In vivo* study.** To characterize acute kidney ischemia injury that occurs before kidney transplantation, we nephrectomized rats and we conserved rinsed kidneys in a conservation solution, namely IGL1, at 4 °C for various periods of time. This experiment in rats promotes cold ischemia similar to that observed in human renal kidneys before transplantation. Adult male Sprague–Dawley rats were assigned to one of five groups of four animals each. Rats were anesthetized with intraperitoneal ketamine. The abdomen was then opened through a midline incision and the kidneys were perfused with cold heparinized saline. Kidneys were next washed with IGL1 followed by incubation in IGL1 during 0 h, 4, 8, 16 and 24 h at 4 °C. All procedures were performed strictly under the Paris Descartes University Animal Care recommendations.

Renal allograft biopsies and immunohistochemistry. In all, 18 preimplantation biopsies were analyzed for GRP78 and NF-κB p65/RelA staining. In all, 15 protocol biopsies performed at 3 months post transplant in stable patients with a normal renal function and who received treatment with tacrolimus, prednisone and mycophenolate mofetil were used as control. Patients wrote informed consent at the time of the transplantation. Pathological examination was strictly normal using Banff scoring. The sections were incubated with an anti-GRP78 rabbit polyclonal antibody or a rabbit anti-NF-κB p65/RelA antibody. The sections were then

incubated with anti-rabbit antibody conjugated to a peroxidase-labeled polymer (Dako, Trappes, France). Details on antibodies are listed on Supplemental Table 2. Tubular GRP78 and NF-κB p65/RelA staining were quantified by dividing the number of positive tubules by the total quantified at $\times 20$ magnification.

Statistical analysis. All data are expressed as means ± S.E.M. of three different experiments, unless otherwise specified. Biological and histological data were compared using non-parametric tests. We used the Mann-Whitney U-test for non-parametric data comparisons between two groups, and the Student's test for parametric data. Statistical analyses were performed using Prism-GraphPad software (GraphPad Prism4, GraphPad Software, La Jolla, CA, USA). A P-values of < 0.05 were considered significant.

Conflict of interest

The authors declare no conflict of interest.

Author's contributions
SF performed all of the experiments; NB performed in vivo studies; DA generated primary cultured cells; CL, ET and PB supervised the project; NP designed the study and wrote the paper.

1. Bonventre J. Diagnosis of acute kidney injury: from classic parameters to new biomarkers. Contrib Nephrol 2007; **156**: 213–219.
2. Nankivell BJ, Chapman JR. Chronic allograft nephropathy: current concepts and future directions. Transplantation 2006; **81**: 643–654.
3. Perico N, Cattaneo D, Sayegh M, Remuzzi G. Delayed graft function in kidney transplantation. Lancet 2004; **364**: 1814–1827.
4. Bonventre J, Zuk A. Ischemic acute renal failure: an inflammatory disease? Kindey Int 2004; **66**: 480–485.
5. Anders H. Toll-like receptors and danger signaling in kidney injury. J Am Soc Nephrol 2010; **21**: 1270–1274.
6. Anders H, Schlondorff D. Innate immune receptors and autophagy: implications for autoimmune kidney injury. Kidney Int 2010; **78**: 29–37.
7. Eddy AA. Molecular basis of renal fibrosis. Pediatr Nephrol 2000; **15**: 290–301.
8. Eddy AA, Neilson EG. Chronic kidney disease progression. J Am Soc Nephrol 2006; **17**: 2964–2966.
9. Leemans J, Stokman G, Claessen N, Rouschop K, Teske G, Kirschning C et al. Renal-associated TLR2 mediates ischemia/reperfusion injury in the kidney. J Clin Invest 2005; **115**: 2894–2903.
10. Wu H, Chen G, Wyburn K, Yin J, Bertolino P, Eris J et al. TLR4 activation mediates kidney ischemia/reperfusion injury. J Clin Invest 2007; **117**: 2847–2859.
11. Zhang K, Kaufman RJ. From endoplasmic-reticulum stress to the inflammatory response. Nature 2008; **454**: 455–462.
12. Lee D, Hung M. All roads lead to mTOR: integrating inflammation and tumor angiogenesis. Cell Cycle 2007; **15**: 3011–3014.
13. Nizet V, Johnson R. Interdependence of hypoxic and innate immune responses. Nat Rev Immunol 2009; **9**: 609–617.
14. Sumpter RJ, Levine B. Autophagy and innate immunity: triggering, targeting and tuning. Semin Cell Dev Biol 2010; **21**: 699–711.
15. Kaufman RJ, Scheuner D, Schroder M, Shen X, Lee K, Liu CY et al. The unfolded protein response in nutrient sensing and differentiation. Nat Rev Mol Cell Biol 2002; **3**: 411–421.
16. Mori K. Tripartite management of unfolded proteins in the endoplasmic reticulum. Cell 2000; **101**: 451–454.
17. Zhang K, Kaufman RJ. Signaling the unfolded protein response from the endoplasmic reticulum. J Biol Chem 2004; **279**: 25935–25938.
18. Xu C, Bailly-Maitre B, Reed JC. Endoplasmic reticulum stress: cell life and death decisions. J Clin Invest 2005; **115**: 2656–2664.
19. Matzinger P. The danger model: a renewed sense of self. Science 2002; **296**: 301–305.
20. Akcay A, Nguyen Q, Edelstein C. Mediators of inflammation in acute kidney injury. Mediators Inflamm 2009; **2009**: 137072.
21. Hayakawa K, Nakajima S, Hiramatsu N, Okamura M, Huang T, Saito Y et al. ER stress depresses NF-kappaB activation in mesangial cells through preferential induction of C/EBP beta. J Am Soc Nephrol 2010; **21**: 73–81.
22. Deng J, Lu P, Zhang Y, Scheuner D, Kaufman R, Sonenberg N et al. Translational repression mediates activation of nuclear factor kappa B by phosphorylated translation initiation factor 2. Mol Cell Biol 2004; **24**: 10161–10168.
23. Kaneko M, Niinuma Y, Nomura Y. Activation signal of nuclear factor-kappa B in response to endoplasmic reticulum stress is transduced via IRE1 and tumor necrosis factor receptor-associated factor 2. Biol Pharm Bull 2003; **26**: 931–935.
24. Urano F, Wang X, Bertolotti A, Zhang Y, Chung P, Harding HP et al. Coupling of stress in the ER to activation of JNK protein kinases by transmembrane protein kinase IRE1. Science 2000; **287**: 664–666.
25. Ron D, Walter P. Signal integration in the endoplasmic reticulum unfolded protein response. Nat Rev Mol Cell Biol 2007; **8**: 519–529.
26. Kuznetsov G, Bush KT, Zhang PL, Nigam SK. Perturbations in maturation of secretory proteins and their association with endoplasmic reticulum chaperones in a cell culture model for epithelial ischemia. Proc Natl Acad Sci USA 1996; **93**: 8584–8589.
27. Montie HL, Kayali F, Haezebrouck AJ, Rossi NF, Degracia DJ. Renal ischemia and reperfusion activates the eIF 2 alpha kinase PERK. Biochim Biophys Acta 2005; **1741**: 314–324.
28. Hung CC, Ichimura T, Stevens JL, Bonventre JV. Protection of renal epithelial cells against oxidative injury by endoplasmic reticulum stress preconditioning is mediated by ERK1/2 activation. J Biol Chem 2003; **278**: 29317–29326.
29. Pallet N, Thervet E, Le Corre D, Knebelmann B, Nusbaum P, Tomkiewicz C et al. Rapamycin inhibits human renal epithelial cell proliferation: effect on cyclin D3 mRNA expression and stability. Kidney Int 2005; **67**: 2422–2433.
30. Livak KJ, Schmittgen TD. Analysis of relative gene expression data using real-time quantitative PCR and the 2(-delta delta C(T)) method. Methods 2001; **25**: 402–408.

Supplementary Information accompanies the paper on Cell Death and Disease website (http://www.nature.com/cddis)